Inclusion Mechanism of Steroid Drugs into β-Cyclodextrins. Insights from Free Energy Calculations

Wensheng Cai,*,† Tingting Sun,† Peng Liu,† Christophe Chipot,‡ and Xueguang Shao†

Department of Chemistry, Nankai University, Tianjin 300071, People's Republic of China, and Equipe de dynamique des assemblages membranaires, UMR CNRS/UHP 7565, Université Henri Poincaré, BP 239, 54506 Vandœuvre-lès-Nancy cedex, France

Received: February 27, 2009; Revised Manuscript Received: April 15, 2009

The inclusion of hydrocortisone, progesterone, and testosterone into the cavity of β-cyclodextrin (β-CD) following two possible orientations was investigated using molecular dynamics simulations and free-energy calculations. The free-energy profiles that delineate the inclusion process were determined using an adaptive biasing force. The present results reveal that although the free-energy surfaces feature two local minima corresponding to a partial and a complete inclusion, the former mode is markedly preferred, irrespective of the orientation. Ranking the propensity of the three steroidal molecules to associate with β-CD, viz. progesterone > testosterone > hydrocortisone, is shown to be in excellent agreement with experiment. This conclusion is further supported by independent calculations relying on alchemical transformations in conjunction with free energy perturbation, wherein the relative binding free energy for the three steroids was estimated. In addition, decomposition of the potentials of mean force into free-energy contributions and significant decrease in the total hydrophobic surface area suggest that by and large, van der Waals and hydrophobic interactions constitute the main driving forces responsible for the formation of the inclusion complexes. Analysis of their structural features from the molecular dynamics trajectories brings to light different hydrogen-bonding patterns that are characterized by distinct dynamics and stabilities.

1. Introduction

Cyclodextrins (CDs), a class of cyclic oligosaccharides, have been the object of considerable attention in pharmaceutical research and development on account of their enhanced aqueous solubility, chemical stability, and bioavailability for a variety of drug molecules through the formation of inclusion complexes.[1] As drug carriers, CDs can be used for improving drug absorption across biological barriers, controlling the rate and time profiles of drug release, or delivering a drug to a targeted site.

Of particular interest, steroids represent an important family of chemical compounds that are involved in a host of biological processes and hence are appropriate candidates for a variety of therapeutic applications. Hydrocortisone (Hyc), a steroidal drug, is a major glucocorticoid and an important intermediate in the synthesis of other steroidal drugs. It has a broad range of anti-inflammatory and immunosuppressive effects and is extensively employed in a large spectrum of therapies.[2] In contrast, progesterone (Pro), is a lipophilic drug used to control reproductive function, as well as in postmenopausal therapy.[3,4] Last, testosterone (Tes) constitutes an important male sex hormone.[5] These three steroid drugs share the common characteristic of a low bioavailability, owing to their poor aqueous solubility. Not too surprisingly, their use in pharmaceutical formulations has been hitherto limited. To overcome this severe shortcoming, CDs and a number of their derivatives have been utilized as effective carriers through the formation of inclusion complexes. The latter are aimed at improving the aqueous solubility of the drug, while enhancing its transport toward a designated target.[6−8] Among the members of the CD family, β-CD, a macrocycle composed of seven repetitive glucose units, and its derivatives represent the best candidates, due to the volume of the cavity that matches the size of the steroids. In the present work, emphasis will be given on the inclusion complexes formed by the three steroidal drugs, viz. Hyc, Pro, and Tes, and β-CD.

On the experimental front, a vast effort has been invested to study the process that governs the formation of the complexes. The association constants and the structure of CD-steroid complexes were determined by solubility measurements, ultraviolet and infrared spectroscopies, and differential thermal analysis.[9−11] The inclusion modes were investigated for several steroid-CD complexes by the NMR spectroscopy[9,12,13] with full and partial inclusion into the β-CD cavity being proposed for Pro and Hyc, respectively. Structural information on the complexes formed by the three steroids with β-CD has been until now somewhat fragmentary. Theoretical approaches have been applied to gain additional, atomic-level insights into the association mechanism, for example, investigation of the interaction of Pro and β-CD by means of steered molecular dynamics (SMD),[14] or the complexation of Hyc by β-CD using molecular mechanical modeling.[15] It, nevertheless, still remains that key issues like the driving forces responsible for complexation, or the underlying free-energy change delineating the reaction ought to be investigated in greater detail to decipher the mechanism whereby steroids and CDs associate.

In the present contribution, inclusion of Hyc, Pro, and Tes with β-CD, following two possible orientations, was investigated using molecular dynamics (MD) simulations and free-energy calculations. The free-energy change along an appropriately chosen reaction pathway was measured for the two selected relative orientations employing an adaptive biasing force (ABF)

* To whom correspondence should be addressed. E-mail: wscai@nankai.edu.cn.
† Nankai University.
‡ Université Henri Poincaré.

10.1021/jp901825w CCC: $40.75
Published on Web 05/08/2009

SCHEME 1: Structures of Hydrocortisone (Hyc), Progesterone (Pro), and Testosterone (Tes)[a]

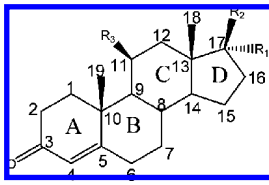

	R_1	R_2	R_3
Hyc	OH	$COCH_2OH$	OH
Pro	H	$COCH_3$	H
Tes	H	OH	H

[a] The carbon atoms of the steroid scaffold are numbered, and the four rings are labeled A, B, C, and D.

scheme,[16−18] as has been used previously to explore other recognition and association processes,[19] as well as transport phenomena.[20−22] To probe the stability of the complexes inferred from the free-energy profiles, the relative binding affinity of the steroids toward β-CD was estimated employing the free energy perturbation (FEP) method in conjunction with the dual-topology paradigm.[23] Noteworthily, it will be shown that these two approaches yield the same affinity ranking in nice agreement with experiment. The driving forces responsible for the formation of the complexes, together with the structural features of the latter at the local minima of the free-energy surface were investigated for each relative orientation, revealing marked differences between Hyc and the two other steroids.

2. Methods

2.1. Molecular Models. Scheme 1 provides a representation of the structure of Hyc, Pro, and Tes. The initial coordinates of β-CD,[24] Hyc, Pro, and Tes were taken form crystal structures available in the protein data bank (pdb code: 2Q1V, 1A28 and 2Q7K). The geometry of these molecules was optimized using a conjugate gradient algorithm. In the subsequent MD simulations, the center of the glycosidic oxygen atoms of β-CD was placed at the origin of the coordinate system, the longitudinal axis of the cavity being arbitrarily collinear with the z direction of Cartesian space. Two possible orientations of the steroids facing the second rim of β-CD were considered - viz. orientation I: A ring, orientation II: D ring, as shown in Scheme 2.

2.2. Developing CHARMM Force Field Parameters. All the simulations reported in this study rely upon the CHARMM27 force field,[25] which has been in large measure developed for proteins, lipids, and nucleic acids. It is, therefore, not too surprising that a number of parameters describing Hyc, Pro, and Tes are missing from the present set of parameters. These parameters were optimized to reproduce quantum-mechanical (QM) data, using the strategies suggested by MacKerell et al.[26,27] Considering the transferability hypothesis and the consistency with the available CHARMM27 force field, only those parameters involved in groups R_1 and R_2 (fragment I), as well as in the A ring (fragment II) were optimized. The geometries and the vibration spectra of the latter fragments were determined at the MP2/6-31G(d) level of approximation, employing the Gaussian 03 suite of programs.[28] Assignment of the frequencies for the empirical and the QM levels of theory was carried out by matching both frequencies and eigenvector projections.[29,30] The conformational energies associated with the isomerization about flexible bonds were also scanned at the MP2/6-31G(d) level of theory and further utilized to optimize the corresponding torsional parameters on the basis of the reproduction of the corresponding QM potential energy surfaces. The new parameters, the comparison of the vibration frequencies, and the fit of the potential energy surfaces are supplied in the Supporting Information.

2.3. Molecular Dynamics Simulations. All simulations were performed using the parallel, scalable MD program NAMD2.6.[31] The carbohydrate solution force field (CSFF)[32] parameters, the newly optimized parameters for steroids, and the existing CHARMM27 parameters were employed to describe the intermolecular interactions. The TIP3P[33] water model was used to model the aqueous solution. The charges of the three steroids were inferred from that of cholesterol.[34] MD simulations of the complexes formed by the steroids and β-CD were performed in the isobaric−isothermal ensemble with periodic boundary conditions. The temperature and the pressure were maintained at 298.15 K and 1 atm, respectively, employing Langevin dynamics and the Langevin piston method.[35] Chemical bonds involving hydrogen atoms were constrained to their experimental lengths by means of the Shake/Rattle algorithms.[36,37] The r-RESPA multiple time-step algorithm was employed to integrate the equations of motion with a time step of 2 and 4 fs for short- and long-range interactions, respectively.[38] These time steps were used in all simulations, unless indicated otherwise. Long-range electrostatic forces were taken into account by means of the particle mesh Ewald (PME) scheme,[39] and a 14 Å cutoff was applied to truncate van der Waals interactions.

2.4. Free Energy Calculations. ***2.4.1. ABF Calculations.*** In the molecular systems, the glycosidic oxygen atoms of β-CD form the first subset of atoms. Atoms O_1 and R_2 of the steroids form the second subset of atoms located on the z-axis, 10 Å away from the origin. The model reaction coordinate, ξ, used here was chosen as the projection onto the z-direction of Cartesian space of the distance separating the latter two subsets of atoms, as shown in Scheme 2. The free-energy profiles delineating the association of the steroids and β-CD along ξ were generated using the ABF method.[16] To keep the central cavity of β-CD centered about the z axis during the MD simulations, the glycosidic oxygen atoms were restrained by means of weak harmonic restraints with a force constant of 1.0 kcal/mol/Å^2. The reaction pathway, spanning -10 Å $\leq \xi \leq +20$ Å, was broken down into 15 consecutive windows 2 Å wide. In each window, a 1.5 ns MD trajectory was generated, hence corresponding to a total simulation time of 22.5 ns. Instantaneous values of the force were accrued in bins 0.1 Å wide. To improve uniformity of the sampling along ξ and continuity of the average force across adjacent windows, the width of the windows was adapted wherever needed, and convergence of the free energy was probed by extending the simulation time to 2 ns in regions featuring barriers and minima.

The initial structures were immersed in a bath of explicit solvent containing ca. 2000 water molecules. A 1 ns equilibrium MD simulation was carried out for each initial molecular assembly as a preamble to the ABF calculations. For the inclusion complexes corresponding to the minima highlighted in the free-energy profiles, 10 ns MD simulations were performed to analyze their structural features.

2.4.2. Free Energy Perturbation (FEP) Calculations. ABF calculations provide the free-energy variation in the course of the inclusion process from whence the stability of the complexes can be estimated. To probe the results supplied by ABF, the FEP method[40] was employed as a route for measuring the relative stability of these complexes. With this objective in mind, two independent thermodynamic cycles were designed to compare binding affinities of Pro, Tes, and Hyc toward β-CD, as sketched in Scheme 3 where $\Delta G_2 - \Delta G_1 = \Delta G_{comp} - \Delta G_{mono}$. Here, ΔG_{mono} and ΔG_{comp} stand for the free-energy changes for mutating the steroid in the free state and in the bound, that is, complex state, respectively. These alchemical

SCHEME 2: Two Orientations of the Steroids Penetrating the β-CD Cavity[a]

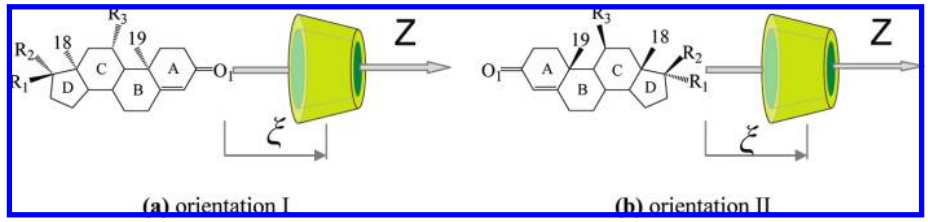

[a] (a) Orientation I and (b) orientation II.

SCHEME 3: Thermodynamic Cycles Used for Estimating the Relative Binding Free Energy of Steroid-β-CD Complexes[a]

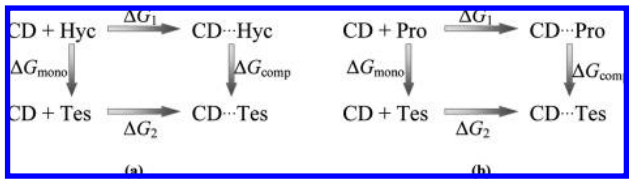

[a] The vertical legs correspond to the "alchemical transformations" in the free state (left) and in the bound state (right). (a) Transformation of Hyc into Tes, (b) transformation of Pro into Tes.

transformations were performed using the FEP formulation in conjunction with the dual-topology paradigm[23] in which the atoms pertaining to both the initial and the final states of the transformation coexist, yet never interact. The initial structures of the complexes utilized for the FEP calculations were extracted from the lowest minima of the ABF profiles, followed by 0.5 ns MD simulations. To improve the accuracy and accelerate the convergence of the FEP calculations, the pathway connecting the reference state of the transformation to the target state was stratified into 132 windows of uneven widths. In particular, toward the end of the transformation, that is, $0.99 < \lambda < 1$, up to 33 windows were utilized to circumvent end-point singularities. In each window, 10 ps of equilibration were followed by 30 ps of data collection, corresponding to a total of 5.28 ns per run. To address the issue of precision versus accuracy,[41,42] each FEP calculation was repeated three times.

3. Results and Discussion

3.1. The ABF Route. The free-energy profiles characterizing the inclusion of the three steroids in β-CD along the *z*-axis are depicted in Figure 1 for orientations I and II. It is clear that for both orientations (i) all the six profiles possess along ξ two marked local minima and a barrier separating them, where the first minima are systematically deeper, and (ii) compared to Pro and Tes, the energy barrier of Hyc is significant higher.

In orientation I, where the A ring of the steroids enters the cavity of β-CD, the free energies decrease sharply to the first local minima around 1.9 Å. Because the A and the B rings are identical for the three steroids, the three curves prior to the first minimum are very similar. Accordingly, the molecular structures corresponding to this minimum are also very similar. As an illustration, the structure of the Hyc-β-CD complex is depicted in Figure 2a. In this complex, the A ring is located inside the cavity and the C_{19} methyl group at the level of the second rim of β-CD. This partial inclusion motif is in good agreement with the ^{1}H NMR experimental results by Uekama et al.[9] According to their studies, it is suggested that the A ring of the steroid is essentially included in the cavity of β-CD.

As the steroids move deeper in the cavity, free-energy barriers emerge on account of steric hindrances caused by the branched groups, viz. C_{19} methyl, R_3, and C_{18} methyl. These functional groups crossing the cavity result in unfavorable free-energy changes. To understand the effect of the steric hindrances on the association process, the geometric changes of the CD cavity were monitored by measuring the average radius of the cavity at the middle level and at the first rim, as shown in Figure 3. The radii displayed in Figure 3a are shown to increase from 2 Å on, which corresponds to the C_{19} methyl group crossing the center of β-CD. The cavity remains oversized until the C_{18} methyl group penetrates the middle of the cavity, viz. around 8.0 Å. Expansion of the first rim when the two methyl groups cross it can also be visualized in the two peaks of Figure 3a. The corresponding steric hindrances at the first peak coincide with the free-energy barrier arising at 4.3 Å; see Figure 1a. This expansion is even magnified in the case of Hyc, due to the R_3 hydroxyl moiety located in the middle of the cavity, as highlighted in Figure 3a, leading to a significant increase of the barrier around 6.0 Å (Figure 1a). The molecular structure corresponding to this stationary point is shown in Figure 2b.

The second glaring free-energy minimum characteristic of orientation I appears around 7.7 Å and corresponds to a deep inclusion structure, wherein the C_{19} methyl protrudes from the cavity and the C_{18} methyl does not reach the middle plane. A representative structure is depicted in Figure 2c. In particular, on account of additional steric hindrances arising from the location of the R_3 hydroxyl group moiety at the primary rim (Figure 3a bottom), as well as the polarity of this moiety, Hyc is characterized by a much higher free energy, compared to the other two steroids. This result may rationalize why in the case of Hyc no deep inclusion mode has been observed at the experimental level.[13] As Hyc moves away from β-CD, the free energy progressively reaches a plateau.

In orientation II, the structure of the complexes at the local minima is shown in Figure 4. Compared to Hyc and Tes, a deeper inclusion complex is formed between Pro and β-CD at the first minimum (Figure 1b). The second minimum of Pro and Tes appears around 5.0 Å when the C_{18} methyl group penetrates the first rim. At variance with the latter two steroids, the pronounced second minimum of Hyc is observed at 8.5 Å. In the corresponding structure shown in Figure 4d, the C_{19} methyl group is located at the primary side and the A ring is buried in the cavity, where it forms favorable van der Waals interactions. In addition, in the case of Hyc, the free-energy barrier at 6.0 Å is smaller than in orientation I. This result stems from the fact that when the R_3 hydroxyl moiety crosses the first rim of the cavity, the C_{19} methyl group has not reached the center of β-CD; hence the steric hindrances involved are not magnified (see Figure 3b).

3.2. Inferring Relative Stability and Preferred Orientation from the Free Energy Profiles. The association constant, K_a, can be obtained by integrating the free-energy profile along ξ to the limit of association.[43,44] When the steroid penetrates within the CD cavity, the sampled volume of configurational space is

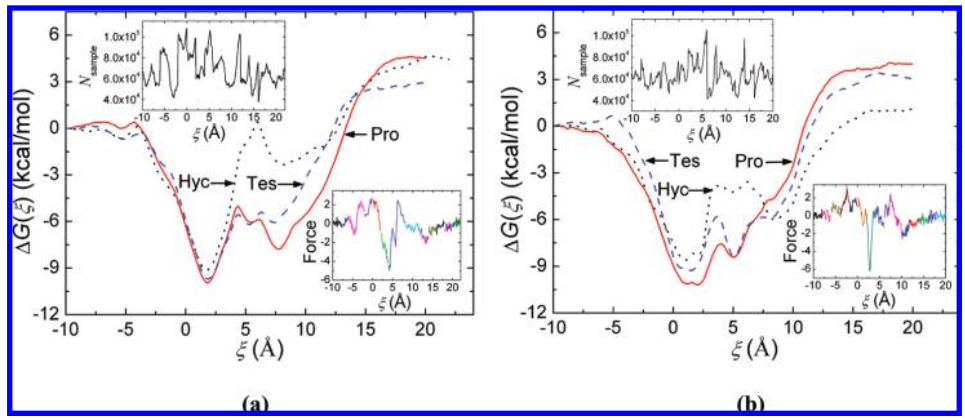

Figure 1. Free energy profiles for the inclusion of steroids into β-CD cavity along the *z* axis in (a) orientation I and (b) orientation II, Hyc (dot line), Pro (solid line), Tes (short dash line). (Inset) number of samples and continuity of force.

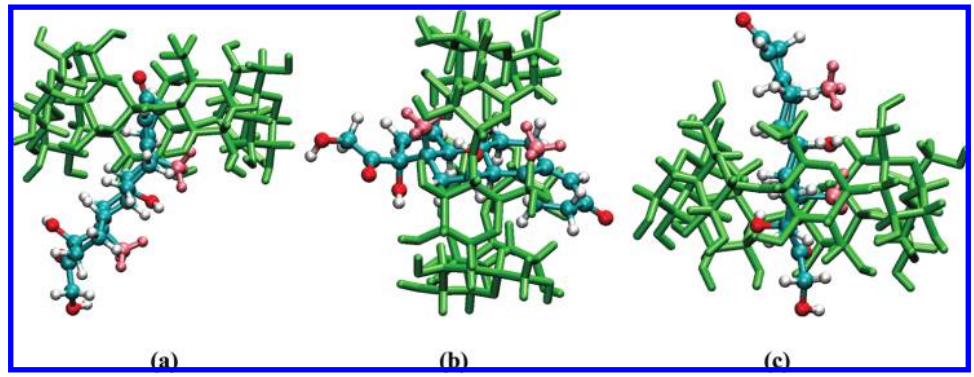

Figure 2. Snapshots of the inclusion complexes of Hyc with β-CD at the inflection points along the free energy curve in orientation I. (a) Near the first minimum, ca. $\xi = 1.9$ Å, (b) near the maximum, ca. $\xi = 6.0$ Å, (c) near the second minimum, ca. $\xi = 7.7$ Å.

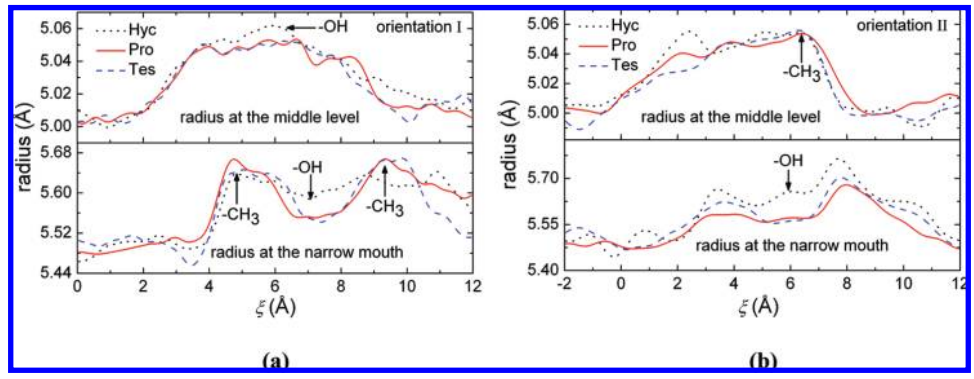

Figure 3. Fluctuation of the radius of the internal cavity as a function of the model reaction coordinate in (a) orientation I, (b) orientation II. (above) Radius in the middle of the cavity, determined by the seven glycosidic oxygen atoms. (below) Radius at the first rim of β-CD, determined by the seven ethyl carbon atoms at the primary side.

restrained to a small cylinder, the cross section of which is defined by the possible (*x*, *y*)-movement of the steroid in the cavity. The association constant was estimated using the equation of ref 44 where the integration is weighted by the surface area of the cross section, and the integration bounds range from −10 Å to the point where the first maximum emerges. The average radius of the area available for the in-plane movement was computed from the trajectories of the center of mass of the steroid in the cavity. The binding free energies are subsequently computed from the expression of K_a and gathered in Table 1. It is apparent that for orientation I, Hyc and Pro possess, respectively, the lowest and the highest binding affinity toward β-CD, which may be ascribed to the dipole moment of the steroid. On the basis of the point charges utilized in the present work, the dipole moment for the optimized structure of Hyc, Pro, and Tes is equal to 5.8, 2.3, and 2.9 D, respectively, pointing roughly from the head O_1 atom to the R_2 group. The dipole moment for β-CD (viz. 5.0∼17.0 D) points from the second rim to the first rim. As the drug enters the cavity in orientation I, its dipole moment therefore is oriented in the opposite direction from that borne by β-CD, thereby lowering the entire dipole moment of the complex. Yet, it should be reminded that in an aqueous solution within the framework of the linear response theory, the stability of molecular systems is expected to increase with the square of the dipole moment, thus rationalizing the affinity ranking measured for the three steroids.[45]

For orientation II, the same affinity ranking is observed from the binding free energies supplied in Table 1. The lowest binding affinity measured for Hyc can be ascribed mainly to unfavorable

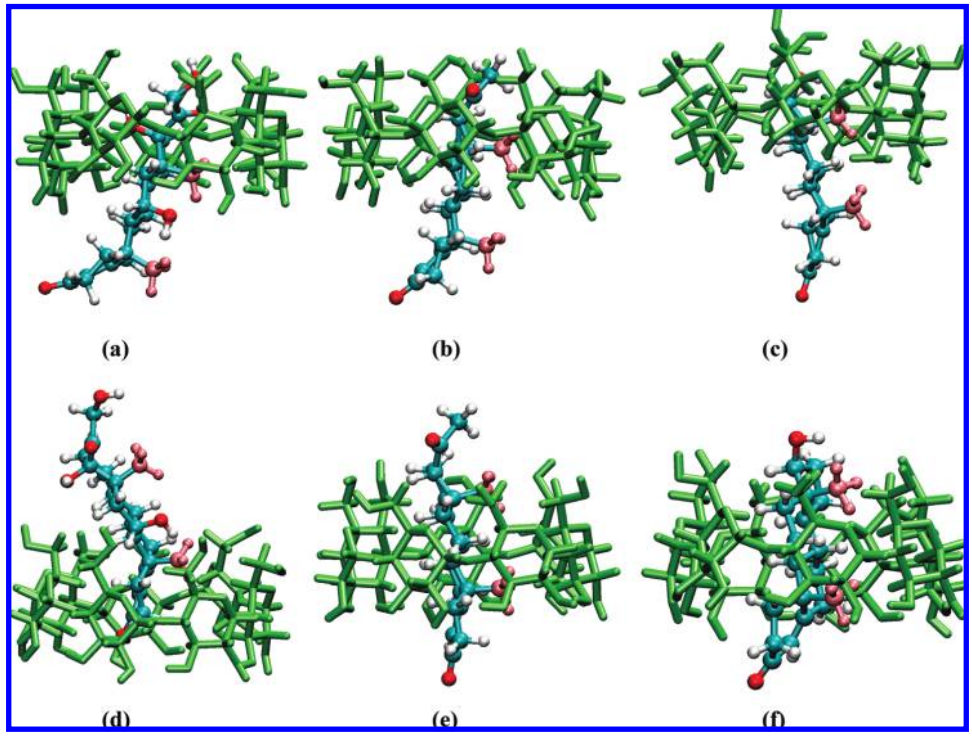

Figure 4. Snapshots of the inclusion complexes formed by the steroids and β-CD at the inflection points of the free-energy profile delineating association in orientation II. (a−c) Near the first minimum: (a) Hyc-β-CD, (b) Pro-β-CD, (c) Tes-β-CD. (d−f) Near the second glaring minimum: (d) Hyc-β-CD, ca. $\xi = 8.5$ Å, (e) Pro-β-CD, ca. $\xi = 5.0$ Å, (f) Tes-β-CD, ca. $\xi = 5.0$ Å.

TABLE 1: Calculated Binding Free Energies ($-\Delta G_{bind\_cal}$) of the Steroids with β-CD (comparison with the experimental estimates ($-\Delta G_{bind\_exp}$))

	$-\Delta G_{bind\_cal}$ (kcal/mol)		
steroid	orientation I	orientation II	$-\Delta G_{bind\_exp}$ (kcal/mol)
Hyc	5.7	5.5	4.4[a]/4.9[b]
Pro	6.6	7.1	5.6[a]
Tes	6.3	6.1	5.3[a]/5.2[c]

[a] From ref 9. [b] From ref 46 and 47. [c] From ref 48.

contacts between the hydrophilic R_1, R_2 groups and the hydrophobic cavity (Figure 4a). On the other hand, the higher binding affinity for Pro, compared to Tes, is due to favorable van der Waals interactions of the hydrocarbon tail with the internal cavity of β-CD (Figure 4b).

Preferred relative orientation of the reactants in the complexation process constitutes a recurrent question. The answer for each steroid can be obtained by comparing ΔG_{bind_cal} for the two orientations considered in this work. For the inclusion of Hyc and Tes with β-CD, orientation I appears to be favored, albeit preference for the latter is less marked. For Pro, however, orientation II is always favored.

In summary, the present ABF calculations show that the relative binding affinity toward β-CD follows the ranking order Pro > Tes > Hyc. From an experimental perspective, the association constant, K_a, has been reported for a variety of CD-steroid complexes in solution by Uekama et al.,[9,46−48] based on thermal analysis. The binding free energies, ΔG_{bind_exp}, are gathered in Table 1. These experimental data indicate that the relative stability of the complexes is comparable to that supplied by the free-energy calculations. However, the latter may not be completely reconciled with the experiment. As a matter of principle, association of a molecule with CD ought to be isotropic. Yet, from a computational standpoint, it is essential to restrain configurational space to ensure that association can be observed over the time scale explored. Enforcing restraints reduces configurational entropy, which has a contribution to the binding free energy. It therefore should be underlined that the calculations reported here do not account for the loss of translational/rotational entropy imposed by the restraints along the chosen reaction coordination to reduce the possibilities for the drug to enter the cavity of β-CD.[49] In addition to this consideration, the difference between ΔG_{bind_cal} for the preferred inclusion mode and the corresponding ΔG_{bind_exp} in Table 1 may also stem from force field imperfections for these steroidal molecules, thus calling for further fine-tuning of the intermolecular potential.

From a structural viewpoint, these calculations reveal that the energetically favored arrangements of Hyc-β-CD and Tes-β-CD are those corresponding to the first local minima with orientation I. This motif characterized by a partial inclusion is in line with the results obtained by NMR, suggesting that the preferred inclusion mode for Hyc-β-CD and Tes-β-CD is when the A ring interacts strongly with the β-CD cavity.[9,12] The steric hindrances caused by the branched groups and unfavorable interactions of the hydrophilic R_1, R_2 groups and the hydrophobic cavity prevent further penetration of Hyc into the latter. At variance with the latter two complexes, no preferred orientation has been determined for Pro-β-CD on the basis of NMR investigations. The present simulations confirm that penetration of the cavity by the D ring represents the most probable orientation, which is in agreement with previous theoretical predictions using SMD numerical experiments.[14]

3.3. FEP Calculations. In an attempt to probe the results obtained from the aforementioned ABF simulations, FEP calculations based on the thermodynamic cycles sketched in Scheme 3 were carried out. In a similar fashion, two possible orientations were considered by means of two independent sets of runs. In the first set, the initial structures of the complexes were taken from the lowest minima of the ABF profiles in

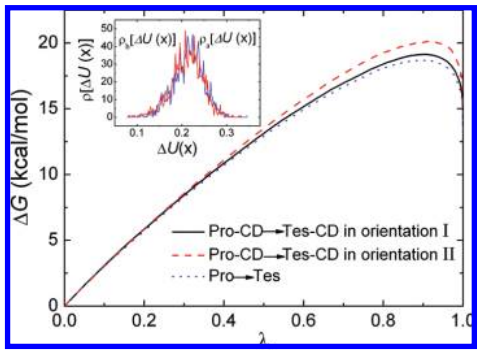

Figure 5. Evolution of the relative free energy, ΔG, as a function of the general extent parameter, λ, in the FEP alchemical transformation of Pro into Tes in the free state and in the bound state for the two chosen orientations. Inset: Typical overlap of configurational ensembles reflected in their respective density of states, $[U(x)]$, characteristic of contiguous intermediate states of the transformation at $\lambda = 0.5$.

TABLE 2: Free Energy Changes Characterizing the Mutation of Pro and Hyc into Tes in the Bound State and in the Free State for the Two Selected Orientations Determined Using FEP[a]

mutation		ΔG_{mono}	ΔG_{comp}	$\Delta\Delta G$
orientation I	Pro→Tes	13.3 ± 0.1	14.0 ± 0.3	0.7 ± 0.3
	Hyc→Tes	−46.1 ± 0.2	−47.1 ± 0.2	−1.0 ± 0.2
orientation II	Pro→Tes	13.3 ± 0.1	14.9 ± 0.1	1.7 ± 0.2
	Hyc→Tes	−46.1 ± 0.2	−46.6 ± 0.3	−0.5 ± 0.3

[a] The error estimate corresponds to the standard deviation over three independent runs (free energies in kcal/mol).

orientation I. In the second set, they were taken from orientation II. For reproducibility purposes, the free-energy change for the transformation in each leg of Scheme 3 was determined from three independent runs.

To assess whether the system has reached equilibrium in the data-collection stage of the FEP calculations, evolution of the free energy with respect to the general extent parameter, λ, was monitored in the course of the transformation, as depicted in Figure 5. The behavior of the free energy as a function of λ and the overlap of the thermodynamic ensembles embodied in their density of states suggest that the necessary conditions for an appropriate convergence of the simulations are met.

The estimated differences in the binding free energies, together with the free-energy changes arising from the point mutations are gathered in Table 2. It is apparent from the latter that the relative stability of the three complexes can be ranked as Pro > Tes > Hyc for both orientations in line with the ABF results. The free-energy changes obtained following two distinct routes, viz. the ABF and FEP methods, are therefore quantitatively consistent, underlining the robustness and the reliability of the present set of calculations. Yet, it is worth noting that a preferred orientation cannot be inferred from FEP calculations alone.

3.4. Driving Forces Responsible for Association. To analyze the driving forces responsible for the binding of the steroids to β-CD, two distinct, viz. short- and long-range interactions were monitored over the entire association process, based on the free-energy profiles. This was achieved by partitioning the total average force acting along the model reaction coordinate into van der Waals drug-CD, electrostatic drug-CD, and drug-solvent components and integrating the latter independently. The resulting free-energy contributions to the inclusion of Hyc and Pro into β-CD are depicted for the two orientations in Figure 6. Because of its resemblance to Pro, the data for Tes is not shown. For orientation I, from the initial position to the first minimum, both van der Waals and electrostatic interactions appear to decrease abruptly. It is suggestive that these forces drive in a cooperative fashion the formation of the most stable inclusion complexes, albeit van der Waals interactions are shown to be predominant. Electrostatic interactions subsequently level off and become nearly constant, fluctuation of the free energy resulting mainly from the van der Waals contribution. In orientation II, a similar trend was observed for Pro. In the case of Hyc, however, the electrostatic interactions appear to play a more important role in the formation of the first-minimum inclusion complex (Figure 6c), the oxygen atoms of R_1 and R_2 interacting favorably with the secondary hydroxyl groups.

Hydrophobic interactions are generally considered to be driving force for CD complexation with highly hydrophobic guest molecules. Experimental studies have shown that the total entropy change for this process is positive.[50] Yet, the subject of hydrophobic interaction itself still remains controversial. Complexation by CDs generally involves disruption and removal of the structured water molecules inside the CD cavity and around the nonpolar guests, and the hydrophobic interactions of nonpolar guests with the hydrophobic CD cavity. Although the corresponding contributions to the association free energy cannot be assessed using the above decomposition method, the desolvation effect can be seen from the increasing steroid-solvent interactions when approaching the cavity, as shown in Figure 6. An alternative approach to highlight how the hydrophobic interactions contribute to CD complexation consists in calculating the changes in the solvent-accessible hydrophobic surface area of the steroids upon complexation with β-CD.[50] Calculations of the nonpolar surface area of the steroids in the free state and the corresponding changes in the complex state were, therefore, carried out using the VEGA ZZ program.[51] The structures of the complexes used for the surface calculations were taken from the lowest minima of the ABF profiles in Figure 1. The results show a significant decrease in the total hydrophobic surface area (ca. 40%) of the steroids for the two orientations, which may stem from the contributions of hydrophobic interactions of the hydrophobic cavity of CD and the hydrophobic steroid skeleton. This also indicates that the latter forces constitute the driving forces responsible for the binding of the steroids to β-CD.[7]

3.5. Structural Analysis of the Inclusion Complexes. To investigate the stability and the structural features of the complexes at the global minimum of the free-energy profiles, additional 10 ns MD simulations were performed for each structure. From the analysis of the trajectories, the variation of the model reaction coordinate, ξ, which is a measure of the relative position of the steroid with respect to β-CD, is reported in Figure 7. For orientation I, it is clear that the Hyc-β-CD and the Tes-β-CD complexes remain relatively steady over the 10 ns time scale. The Pro-β-CD complex is essentially unaltered within a 10 ns MD simulation, although transition toward the second minimum is observed after 7 ns. For orientation II, the Hyc-β-CD complex still exhibits the greatest stability, compared to Pro and Tes. Pro and Tes are shown to be able to translocate from the first minimum to the second minimum as a result of the small and narrow barriers in the free-energy profiles. For the Pro-β-CD complex, the second minimum that corresponds to the deep inclusion mode is likely to be observed in experiments, although the first minimum in orientation II is the energetically preferred inclusion mode, as has been reported in ref 13.

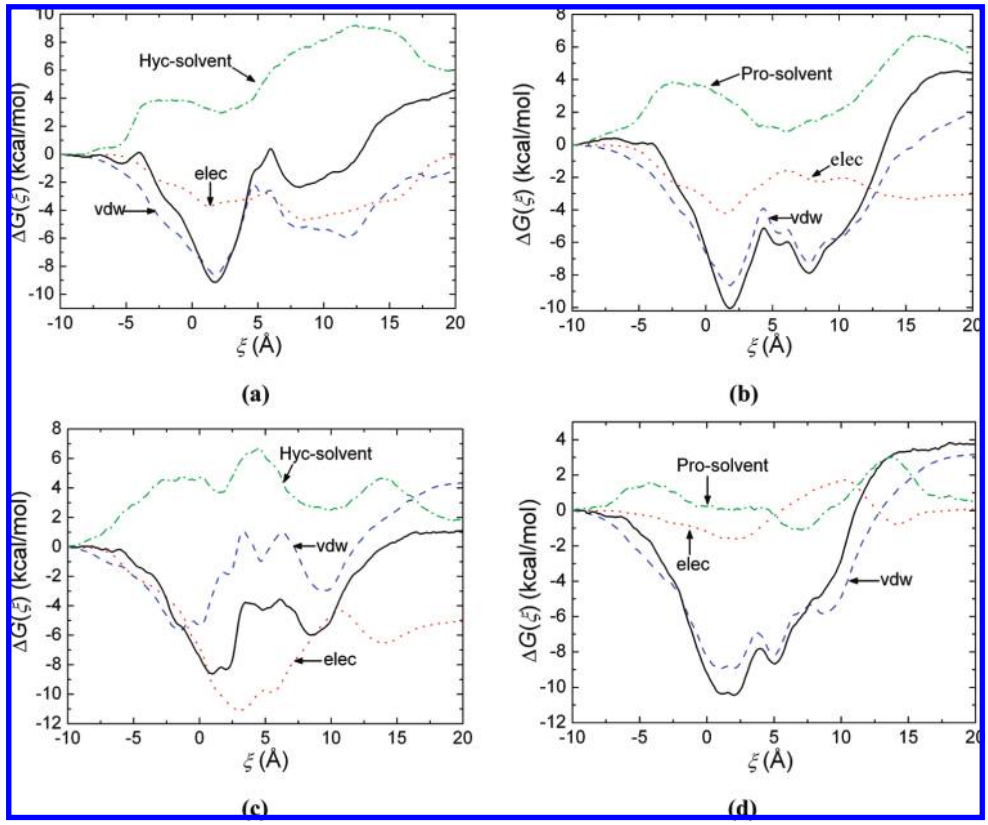

Figure 6. Partition of the total association free energy (solid line) into van der Waals steroid-CD (dashed line), electrostatic steroid-CD (dotted line), and steroid-solvent (dotted-dashed line) contributions. (a) Hyc in orientation I, (b) Pro in orientation I, (c) Hyc in orientation II, (d) Pro in orientation II.

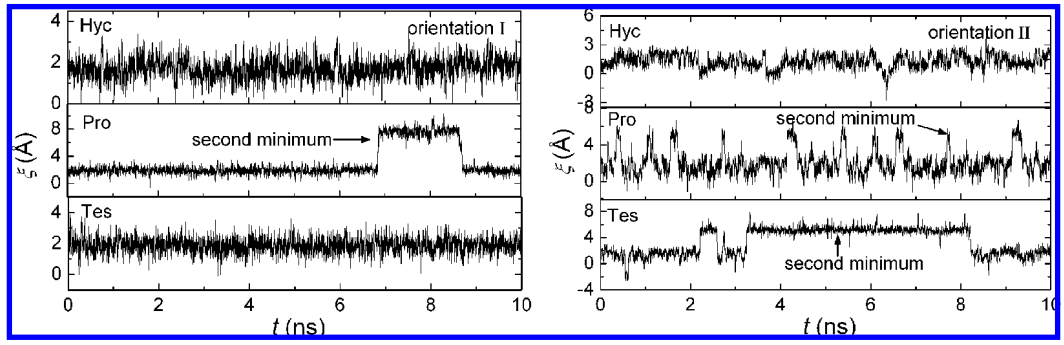

Figure 7. Variations of ξ obtained from the MD trajectories of the complexes at the global minimum of the free energy profiles.

The hydrogen bonds formed between the steroids and β-CD were analyzed from the trajectories. Intermolecular hydrogen bonds were found in Hyc-β-CD complex, regardless of the orientation (see Figure 3S in Supporting Information), but seldom in both Pro- and Tes-β-CD complexes. In the Hyc-β-CD complex with orientation I, the hydrogen bonds are formed between the R_3 or R_1 hydroxyl group of Hyc and the secondary hydroxyl group of β-CD. For orientation II, the hydroxyl moieties of R_2 and R_3 are involved in the formation of hydrogen bonds with the primary and secondary rim of β-CD, respectively. In the Pro-β-CD complex with orientation II, over a 10 ns time scale, the carbonyl group of C_{20} is only engaged in a limited number of hydrogen bonds with the primary hydroxyl group of β-CD.

4. Conclusions

Free-energy calculations characterizing the inclusion of three steroidal drugs, viz. Hyc, Pro, and Tes, into β-CD, following two possible relative orientations, have been carried out, employing ABF[16−18] and FEP[52] methods. The two theoretical approaches yield an identical affinity ranking for the binding of the three steroids to β-CD, in line with experimental observations.[9,46−48] In the light of the analysis of the free-energy profiles determined using the ABF method along the chosen model reaction coordinate, orientation I is suggested to be favored for Hyc and Tes, albeit orientation II appears to be favored for Pro. Moreover, van der Waals and hydrophobic interactions are shown to constitute the main driving forces responsible for the inclusion process in the preferred orientation. Additional MD simulations of the complexes at the global minimum of the free-energy surface were also performed. Analysis of the trajectories suggests that in contrast with Hyc-β-CD and Tes-β-CD, transition between the most thermodynamically stable structure of Pro-β-CD (Figure 4b) and the second stable structure (Figure 4e) can be witnessed. Moreover, comparison between the three steroids reveals that the side chain

of these molecules plays a significant role in their complexation by β-CD in an aqueous environment.

It is expected that the new insights gained from the free-energy calculations proposed in this study will contribute to improve our understanding of the molecular mechanisms that underlie the formation of CD-mediated steroidal drug carriers. Recently, new CD derivatives, viz. functionalized CDs with an amphiphilic tail,[53] have been envisioned to act as vectors for the assisted transport of steroids across the biological membrane, toward their designated target, thereby improving their bioavailability. In this sense, the present work opens exciting perspectives and paves the way for future investigations aimed at the design of drug carrier systems based on functionalized CDs.

Acknowledgment. This study was supported by National Natural Scientific Foundation of China (No. 20873066), and also by Nankai University ISC. C.C. acknowledges the French Embassy in Beijing for travel support.

Supporting Information Available: New CHARMM-based force field parameters developed for two fragment molecules included in hydrocortisone. Comparison of the CHARMM calculated vibration frequencies and potential-energy curves with those determined at the MP2/6-31G(d) level of theory. This material is available free of charge via the Internet at http://pubs.acs.org.

References and Notes

(1) Szejtli, J. *Chem. Rev.* **1998**, *98*, 1743–1753.
(2) Fernandez, J.; Escorsell, A.; Zabalza, M.; Felipe, V.; Navasa, M.; Mas, A.; Lacy, A. M.; Gines, P.; Arroyo, V. *Hepatology* **2006**, *44*, 1288–1295.
(3) Buntner, B.; Nowak, M.; Kasperczyk, J.; Ryba, M.; Grieb, P.; Walski, M.; Dobrzynski, P.; Bero, M. *J. Controlled Release* **1998**, *56*, 159–167.
(4) Latha, M. S.; Lal, A. V.; Kumary, T. V.; Sreekumar, R.; Jayakrishnan, A. *Contraception* **2000**, *61*, 329–334.
(5) McLaren, D.; Siemens, D. R.; Izard, J.; Black, A.; Morales, A. *BJU Int.* **2008**, *102*, 1142–1146.
(6) Sigurdsson, H. H.; Magnusdottir, A.; Masson, M.; Loftsson, T. *J. Inclusion Phenom. Macrocyclic Chem.* **2002**, *44*, 163–167.
(7) Wallimann, P.; Marti, T.; Fürer, A.; Diederich, F. *Chem. Rev.* **1997**, *97*, 1567–1608.
(8) Duchene, D.; Wouessidjewe, D.; Ponchel, G. *J. Controlled Release* **1999**, *62*, 263–268.
(9) Uekama, K.; Fujinaga, T.; Hirayama, F.; Otagiri, m.; Yamasaki, M. *Int. J. Pharm.* **1982**, *10*, 1–15.
(10) Liu, F. Y.; Kildsig, D. O.; Mitra, A. K. *Pharm. Res.* **1990**, *7*, 869–873.
(11) Zarzycki, P. K.; Ohta, H.; Saito, Y.; Jinno, K. *Anal. Bioanal. Chem.* **2008**, *391*, 2793–2801.
(12) Forgo, P.; Vincze, I.; Kover, K. E. *Steroids* **2003**, *68*, 321–327.
(13) Forgo, P.; Gondos, G. *Monatsh. Chem.* **2002**, *133*, 101–106.
(14) Caballero, J.; Zamora, C.; Aguayo, D.; Yanez, C.; Gonzalez-Nilo, F. D. *J. Phys. Chem. B* **2008**, *112*, 10194–10201.
(15) Al-Sou'od, K. A. *J. Solution Chem.* **2008**, *37*, 119–133.
(16) Darve, E.; Pohorille, A. *J. Chem. Phys.* **2001**, *115*, 9169–9183.
(17) Rodriguez-Gomez, D.; Darve, E.; Pohorille, A. *J. Chem. Phys.* **2004**, *120*, 3563–3578.
(18) Hénin, J.; Chipot, C. *J. Chem. Phys.* **2004**, *121*, 2904–2914.
(19) Yu, Y. M.; Chipot, C.; Cai, W. S.; Shao, X. G. *J. Phys. Chem. B* **2006**, *110*, 6372–6378.
(20) Gorfe, A. A.; Babakhani, A.; McCammon, J. A. *Angew. Chem., Int. Ed.* **2007**, *46*, 8234–8237.
(21) Dehez, F.; Pebay-Peyroula, E.; Chipot, C. *J. Am. Chem. Soc.* **2008**, *130*, 12725–12733.
(22) Spiegel, K.; Magistrato, A.; Carloni, P.; Reedijk, J.; Klein, M. L. *J. Phys. Chem. B* **2007**, *111*, 11873–11876.
(23) Gao, J.; Kuczera, K.; Tidor, B.; Karplus, M. *Science* **1989**, *244*, 1069–1072.
(24) Lindner, K.; Saenger, W. *Carbohydr. Res.* **1982**, *99*, 103–115.
(25) MacKerell, A. D., Jr.; Bashford, D.; Bellott, R. L.; Dunbrack, R. L., Jr.; Evanseck, J. D.; Field, M. J.; Fischer, S.; Gao, J.; Guo, H.; Ha, S.; Joseph-McCarthy, D.; Kuchnir, L.; Kuczera, K.; Lau, F. T. K.; Mattos, C.; Michnick, S.; Ngo, T.; Nguyen, D. T.; Prodhom, B.; Reiher, W. E., III.; Roux, B.; Schlenkrich, M.; Smith, J. C.; Stote, R.; Straub, J.; Watanabe, M.; Wiorkiewicz-Kuczera, J.; Yin, D.; Karplus, M. *J. Phys. Chem. B* **1998**, *102*, 3586–3616.
(26) Pavelites, J. J.; Gao, J. L.; Bash, P. A.; Mackerell, A. D. *J. Comput. Chem.* **1997**, *18*, 221–239.
(27) Foloppe, N.; MacKerell, A. D. *J. Comput. Chem.* **2000**, *21*, 86–104.
(28) Frisch, M. J.; Trucks, G. W.; Schlegel, H. B.; Scuseria, G. E.; Robb, M. A.; Cheeseman, J. R.; Montgomery, J. A., Jr.; Vreven, T.; Kudin, K. N.; Burant, J. C.; Millam, J. M.; Iyengar, S. S.; Tomasi, J.; Barone, V.; Mennucci, B.; Cossi, M.; Scalmani, G.; Rega, N.; Petersson, G. A.; Nakatsuji, H.; Hada, M.; Ehara, M.; Toyota, K.; Fukuda, R.; Hasegawa, J.; Ishida, M.; Nakajima, T.; Honda, Y.; Kitao, O.; Nakai, H.; Klene, M.; Li, X.; Knox, J. E.; Hratchian, H. P.; Cross, J. B.; Bakken, V.; Adamo, C.; Jaramillo, J.; Gomperts, R.; Stratmann, R. E.; Yazyev, O.; Austin, A. J.; Cammi, R.; Pomelli, C.; Ochterski, J. W.; Ayala, P. Y.; Morokuma, K.; Voth, G. A.; Salvador, P.; Dannenberg, J. J.; Zakrzewski, V. G.; Dapprich, S.; Daniels, A. D.; Strain, M. C.; Farkas, O.; Malick, D. K.; Rabuck, A. D.; Raghavachari, K.; Foresman, J. B.; Ortiz, J. V.; Cui, Q.; Baboul, A. G.; Clifford, S.; Cioslowski, J.; Stefanov, B. B.; Liu, G.; Liashenko, A.; Piskorz, P.; Komaromi, I.; Martin, R. L.; Fox, D. J.; Keith, T.; Al-Laham, M. A.; Peng, C. Y.; Nanayakkara, A.; Challacombe, M.; Gill, P. M. W.; Johnson, B.; Chen, W.; Wong, M. W.; Gonzalez, C.; Pople, J. A. *Gaussian 03*; rev. C.02; Gaussian: Wallingford, CT, 2004.
(29) Vaiana, A. C.; Cournia, Z.; Costescu, I. B.; Smith, J. C. *Comput. Phys. Commun.* **2005**, *167*, 34–42.
(30) Scott, A. P.; Radom, L. *J. Phys. Chem.* **1996**, *100*, 16502–16513.
(31) Phillips, J. C.; Braun, R.; Wang, W.; Gumbart, J.; Tajkhorshid, E.; Villa, E.; Chipot, C.; Skeel, R. D.; Kalé, L.; Schulten, K. *J. Comput. Chem.* **2005**, *26*, 1781–1802.
(32) Kuttel, M. M.; Brady, J. W.; Naidoo, K. J. *J. Comput. Chem.* **2002**, *23*, 1236–1243.
(33) Jorgensen, W. L.; Chandrsekhar, J.; Madura, J. D.; Impey, R. W.; Klein, M. L. *J. Chem. Phys.* **1983**, *79*, 926–935.
(34) Pitman, M. C.; Suits, F.; MacKerell, A. D., Jr.; Feller, S. E. *Biochemistry* **2004**, *43*, 15318–15328.
(35) Feller, S. E.; Zhang, Y.; Pastor, R. W.; Brooks, B. R. *J. Chem. Phys.* **1995**, *103*, 4613–4621.
(36) Ryckaert, J. P.; Ciccotti, G.; Berendsen, H. J. C. *J. Comput. Phys.* **1977**, *23*, 327–341.
(37) Andersen, H. C. *J. Comput. Phys.* **1983**, *52*, 24–34.
(38) *Computer Simulation of Liquids*; Allen, M. P.; Tildesley, D. J., Eds.; Clarendon: Oxford, 1987.
(39) Darden, T.; York, D.; Pedersen, L. *J. Chem. Phys.* **1993**, *98*, 10089–10092.
(40) *Free Energy Calculations - Theory and Applications in Chemistry and Biology*; Chipot, C.; Pohorille, A., Eds.; Springer-Verlag: Berlin, 2007.
(41) Lu, N. D.; Kofke, D. A. Modeling. *J. Chem. Phys.* **2001**, *114*, 7303–7311.
(42) Lu, N. D.; Kofke, D. A. *J. Chem. Phys.* **2001**, *115*, 6866–6875.
(43) Shoup, D.; Szabo, A. *Biophys. J.* **1982**, *40*, 33–39.
(44) Auletta, T.; de Jong, M. R.; Mulder, A.; van Veggel, F. C. J. M.; Huskens, J.; Reinhoudt, D. N.; Zou, S.; Zapotoczny, S.; Schonherr, H.; Vancso, G. J.; Kuipers, L. *J. Am. Chem. Soc.* **2004**, *126*, 1577–1584.
(45) Onsager, L. *J. Am. Chem. Soc.* **1936**, *58*, 1486–1493.
(46) Szeman, J.; Ueda, H.; Szejtli, J.; Fenyvesi, E.; Machida, Y.; Nagai, T. *Chem. Pharm. Bull.* **1987**, *35*, 282–288.
(47) Szeman, J.; Fenyvesi, E.; Szejtli, J.; Ueda, H.; Machida, Y.; Nagai, T. *J. Inclusion Phenom.* **1987**, *5*, 427–431.
(48) Szejtli, J. *J. Inclusion Phenom. Mol. Recognit. Chem.* **1992**, *14*, 25–36.
(49) Dixit, S. B.; Chipot, C. *J. Phys. Chem. A* **2001**, *105*, 9795–9799.
(50) Liu, L.; Guo, Q. X. *J. Inclusion Phenom. Macrocyclic Chem.* **2002**, *42*, 1–14.
(51) Pedretti, A.; Villa, L.; Vistoli, G. *J. Comput.-Aided Mol. Des.* **2004**, *18*, 167–173.
(52) Zwanzig, R. W. *J. Chem. Phys.* **1954**, *22*, 1420–1426.
(53) Javierre, I.; Nedyalkov, M.; Petkova, V.; Benattar, J. J.; Weisse, S.; Auzely-Velty, R.; Djedaini-Pilard, F.; Perly, B. *J. Colloid Interface Sci.* **2002**, *254*, 120–128.

JP901825W